Journal of ELECTRONIC MATERIALS, Vol. 46, No. 7, 2017
DOI: 10.1007/s11664-017-5433-9
© 2017 The Minerals, Metals & Materials Society

$Li_n@B_{36}$ (n = 1, 2) Nanosheet with Remarkable Electro-Optical Properties: A DFT Study

MOHAMMAD SOLIMANNEJAD,[1,2,4] SAEEDEH KAMALINAHAD,[1,2] and EHSAN SHAKERZADEH[3]

1.—Department of Chemistry, Faculty of Science, Arak University, Arāk 38156-8-8349, Iran. 2.—Institute of Nanosciences and Nanotechnology, Arak University, Arāk 38156-8-8349, Iran. 3.—Chemistry Department, Faculty of Science, Shahid Chamran University of Ahvaz, Ahvaz, Iran. 4.—e-mail: m-solimannejad@araku.ac.ir

In this study, an attempt has been made to investigate alteration in electro-optical properties of bowl-shape B_{36} nanosheet due to interaction with one and two Li atoms. Our results reveal that the highest occupied molecular orbital–lowest unoccupied molecular orbital (HOMO–LUMO) gap of B_{36} nanosheet is decreased because of a high energy level which is formed under influence of interactions with Li atoms. Gigantic enhancement in the first hyperpolarizability (β_0) of the studied nanosheet up to 4920.62 au is indicated owing to the effect of Li adsorption. The result of the present study may be eventuating to design and fabrication of a nanosheet with tunable electro-optical properties.

Key words: Bowl-shape B_{36} nanosheet, DFT, hyperpolarizability, NLO

INTRODUCTION

Due to broad applications of nonlinear optical (NLO) materials in optical communication, optical computing, telecommunications, information storage and optical switching devices, design of promising high-efficiency NLO materials is an important task in contemporary physical chemistry researches.[1–16] It is known that the species involving the excess electron can display the significant NLO response, where the excess electron plays a crucial role in increasing the first hyperpolarizability (β_0).[17–26]

Inorganic fullerene-like structures have been used in many types of research.[27–29] The new group of cage molecules has been formed from stable fullerene-like boron. Planar or quasi-planar boron clusters at large size were confirmed by experimental and computational analysis.[30–35] Among quasi-planar all-boron layers with a central hexagonal hole, B_{36} is the most stable cluster with C_6v symmetry.[33] Recently, borophene (B_{36}) has been synthesized by Piazza et al.[33] The strongly bound atoms of B_{36} enhance its resistance to mechanical impact. This nanostructure has potential to have an important role in future thin film technology and two-dimensional materials research. Planar boron sheets along with hexagonal vacancies are made from this extended cluster.[36–38] These structures can serve as potential basic parts for fabrication of the hybrid nanostructures with properties.

Recently, it has been shown that B_{40} fullerene interacting with alkali metals could be a potential promising NLO nanomaterial.[39] The main contribution of the present study is to investigate the influence of interaction of the lithium atoms with the bowl-shape B_{36} nanosheet on its electro-optical features. Since boron nanomaterials have unique physiochemical properties, the result of the present study may be eventuating to design and fabrication of a nanosheet with tunable electro-optical properties.

COMPUTATIONAL DETAILS

The geometries of the intended structures are fully optimized using the dispersion-corrected density functional theory B3LYP-D3[40,41] method with the 6-31G(d) basis set. The nature of the stationary points is inspected by frequency analysis at a similar computational level. The geometry

(Received November 17, 2016; accepted March 1, 2017; published online March 15, 2017)

optimization, electronic structure and NLO properties of $Li_n@B_{36}$ with n = 1 and 2 was qualified by the spin-unrestricted approach, whereas the restricted approach was applied to the isolated B_{36} sheet. The correlated S^2 values are about 0.759–0.762 for multiplicity 2, and 2.014 for multiplicity 3 in the $Li@B_{36}$ and $Li_2@B_{36}$ structures, respectively. These results are very similar to the value of 0.750 and 2, respectively, for the pure doublet and triplet states. Therefore, the spin contamination is insignificant and the computational results are reliable. It is significant that selecting a suitable method to calculate the hyperpolarizability of a system is a challenging task. The M06-2X functional is a high-nonlocality functional with double the quantity of nonlocal exchange (2X) to contemplate dispersion forces.[42] The hybrid M06-2X functional is appropriate for use in many nanoscale molecular systems due to a higher percentage of Hartree–Fock (HF) exchange (54%).[25,43,44] The first hyperpolarizability has been evaluated by the finite field (FF) approach under an electric field magnitude of 0.001 a.u., utilizing M06-2X functional with 6-311+G(d) and 6-311+G(2df) basis sets for boron and lithium atoms, respectively. All calculations are performed using Gaussian 09 quantum chemistry code[45] with default convergence criteria.

The highest occupied molecular orbital–lowest Unoccupied molecular orbital (HOMO–LUMO) gap (HLG) of the intended structures is explained as:

$$\mathrm{HLG} = (\varepsilon_L - \varepsilon_H) \quad (1)$$

where ε_H is the HOMO energy and ε_L is the LUMO energy. Also, for intended systems, density of states (DOS) analysis was performed employing the GaussSum program.[46] The system energy in the weak and homogeneous electric field can be shown as[47,48]:

$$E = E^0 - \mu_i F_i - \frac{1}{2}\alpha_{ij}F_iF_j - \frac{1}{6}\beta_{ijk}F_iF_jF_k - \cdots \quad (2)$$

where E^0 and F_i are the molecular total energy without the electric field and the electric field component along the i direction, respectively. The μ_i, α_{ij} and β_{ijk} denote dipole, polarizability, and the first hyperpolarizability, respectively. The magnitude of the total first hyperpolarizability (β_0), a scalar quantity distinguished as a NLO response coefficient, is assessed using these components according to the following equations.

$$\beta_0 = \left(\beta_x^2 + \beta_y^2 + \beta_z^2\right)^{1/2} \quad (3)$$

in which

$$\beta_i = \frac{3}{5}\left(\beta_{iii} + \beta_{ijj} + \beta_{ikk}\right) \quad i,j,k = X,Y,Z \quad (4)$$

The interaction energy (E_{int}) due to the interaction of nanosheet with Li atom is obtained as:

$$E_{int} = E_{Li_n@B_{36}} - E_{B_{36}} - nE_{Li} - E_{BSSE} \quad n = 1,2 \quad (5)$$

where $E_{Li_n@B_{36}}$ represents the total electronic energy of the $Li_n@B_{36}$. The term $E_{B_{36}}$ and E_{Li} are the total electronic energy of isolated B_{36} nanosheet and the Li atom, respectively. To consider basis set superposition error (BSSE) in the computation of the interaction energy, E_{BSSE} is calculated using a counterpoise method.[49]

RESULTS AND DISCUSSIONS

The structure of bowl-shape B_{36} nanosheet is fully optimized at the B3LYP-D3/6-31G(d) level of theory and depicted in Fig. 1a. The pristine B_{36} with C_6v symmetry shows a bowl shape consisting of an out-of-plane distortion. There are three types of boron atoms in B_{36} nanosheet. Six "hub" boron atoms (Bh), the innermost boron atoms on the six-member ring; eighteen "rim" boron atoms (Br) and twelve "bridge" boron atoms (Bb). The bowl B_{36} has two various kinds of foreign B–B distances, 1.58 Å and 1.67 Å. The obtained results are in accordance with previous theoretical reports on the B_{36} nanosheet.[33] The HOMO (ε_H) and the LUMO (ε_L) energies, and the HLG are shown in Table I. DOS and graphic presentation of the HOMO–LUMO distribution of pristine B_{36} are present in Fig. 1b. The HOMO orbital principally acts as an electron donor, and the LUMO orbital mainly acts as an electron acceptor. The obtained HLG for the B_{36} is about 1.916 eV (Table I). Moreover, the NLO properties of B_{36} nanosheet are also investigated at the M062X/6-311+G(d) level of theory and summarized in Table I. The negligible first hyperpolarizability of B_{36} implies naught NLO response of B_{36}.

Li atoms have been considered to be adsorbed on the surface of the pristine B_{36}. Some various initial adsorption sites are selected including atop of different boron atom and B–B bonds, and in concave and convex positions of the nanosheet. The structures of the considered systems are fully optimized at the B3LYP-D3/6-31G(d) level of theory. The obtained stable structures with all real vibrational frequencies and interaction distances are shown in Fig. 2. In these structures, the interaction distances are about 2.133–2.395 Å. In addition, Li adsorption causes elongation of the B–B bonds. The Li adsorption leads to structural deformation of the nanosheet and this could affect the electro-optical features of the considered systems. The calculated E_{int} values for these structures using Eq. 5 are listed in Table I. Based on the results of this table, the negative values of E_{int} indicate that the obtained structures are stable. The E_{int} values are ranging from −1.54 eV to −1.84 eV for $Li@B_{36}$ and −3.42 eV to −3.90 eV for $Li_2@B_{36}$. The obtained results indicate that the complexation of lithium with B_{36} nanosheet is favorable and the Li atom significantly interacts with the surface of this nanosheet.

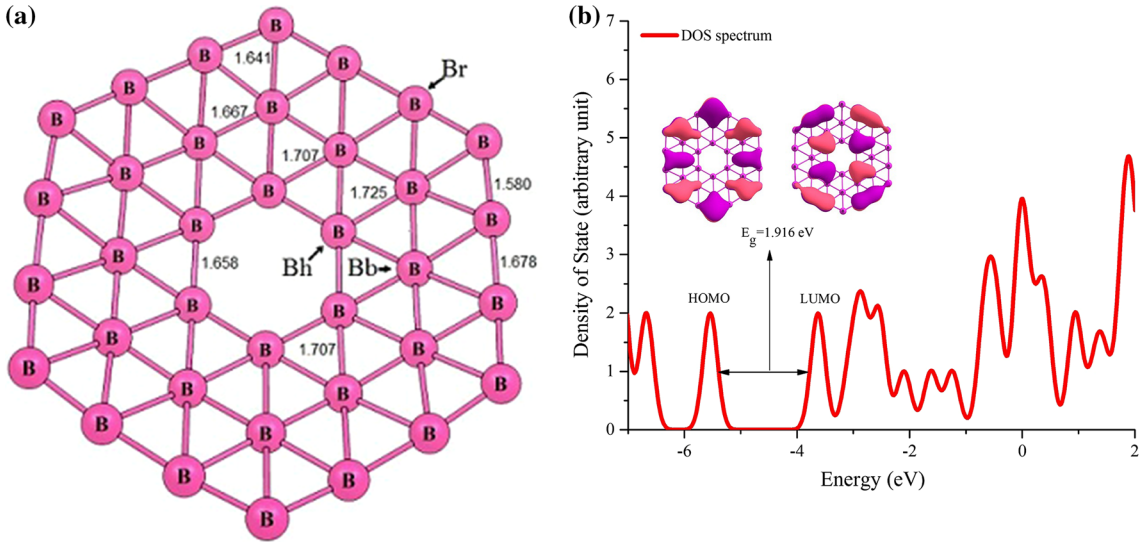

Fig. 1. (a) The optimized geometry and (b) density of states (DOS) of pristine B_{36} nanosheet.

Table I. The frontier molecular orbital energy (ε_H and ε_L), HOMO–LUMO gap (HLG), the energy of the basis set superposition error (E_{BSSE}), the corrected interaction energy (E_{int}) and relative energy values (all in eV), the percentage of variation of HLG (%ΔHLG) together with dipole moment (μ), polarizability (α) and first hyperpolarizability (β_0) values in a.u and charge of lithium atom (|e|)

Structures	Spin multiplicity	ε_H	ε_L	HLG	%ΔHLG[a]	μ	α	β_0	E_{BSSE}	E_{int}	Relative energy	Q_T
Pristine B_{36}	1	−5.534	−3.618	1.916	–	0.84	592.40	75.45	–	–	–	–
A	2	−4.462	−3.497	0.965	−49.62	4.80	640.86	4920.62	0.08	−1.54	0.30	0.896
B	1	−4.725	−3.532	1.193	−37.74	4.11	630.95	1532.98	0.16	−3.42	0.48	0.834
C	2	−4.569	−3.599	0.970	−49.37	2.74	616.72	1008.61	0.09	−1.74	0.09	0.896
D	1	−4.732	−3.580	1.152	−39.88	1.49	622.94	667.30	0.20	−3.68	0.18	0.827
E	2	−4.688	−3.689	0.999	−47.86	0.94	609.37	205.19	0.10	−1.73	0.10	0.860
F	2	−4.655	−3.660	0.996	−48.02	2.41	614.52	195.54	0.08	−1.81	0.03	0.849
G	1	−4.882	−3.785	1.097	−42.76	1.66	616.97	100.12	0.17	−3.90	0	0.882
H	2	−4.628	−3.674	0.953	−50.23	0.02	603.51	74.17	0.08	−1.84	0	0.925
I	3	−4.822	−3.807	1.016	−46.968	1.65	623.42	13.02	0.17	−3.86	0.04	0.882

These structures are arranged in order of decreasing in beta values.[a]The negative signs correspond to a decrease of the HLG with respect to B_{36} nanosheet.

Natural bond orbital (NBO) analysis[50] is also carried out. The NBO charges are listed in Table I. The results presented in Table I indicate that the studied Li atom clusters display positive charge, which exhibits the charge transfer from the Li atom to B_{36} in all of the considered structures. It is clear that the charges of the Li atom are very closed to +1, which demonstrates that the 2s valence electron of the Li atom is ionized; therefore, the lithium salt is formed. As it is expected, the diffuse excess electron of Li atom transfers to the B_{36} which can alter the electronic and NLO properties of the considered system. Furthermore, the NBO analysis in terms of the natural electron configuration is applied to describe the bonding. The natural electron configurations of the considered structures are summarized in Table II. According to the results presented in this table, by adsorption of the lithium atom on the surface of the pristine B_{36}, the p-character of Li atom in the Li···B interaction of the considered system are increased significantly, which indicates the elongation of Li···B interaction proportional to the enhancement of p-character.

The results of frontier molecular orbital energies (ε_H,ε_L) and the HLG energy values for the considered structures are gathered in Table I. According to this table, it is found that the adsorption process narrows the width of the HLG of pristine B_{36} in the range of 0.723–0.963 eV for the Li and Li_2@B_{36} nanosheets, respectively. Thus, HLG values of B_{36} nanosheet are sensitive to the Li adsorption. Among the considered complexes, structure **A** indicates

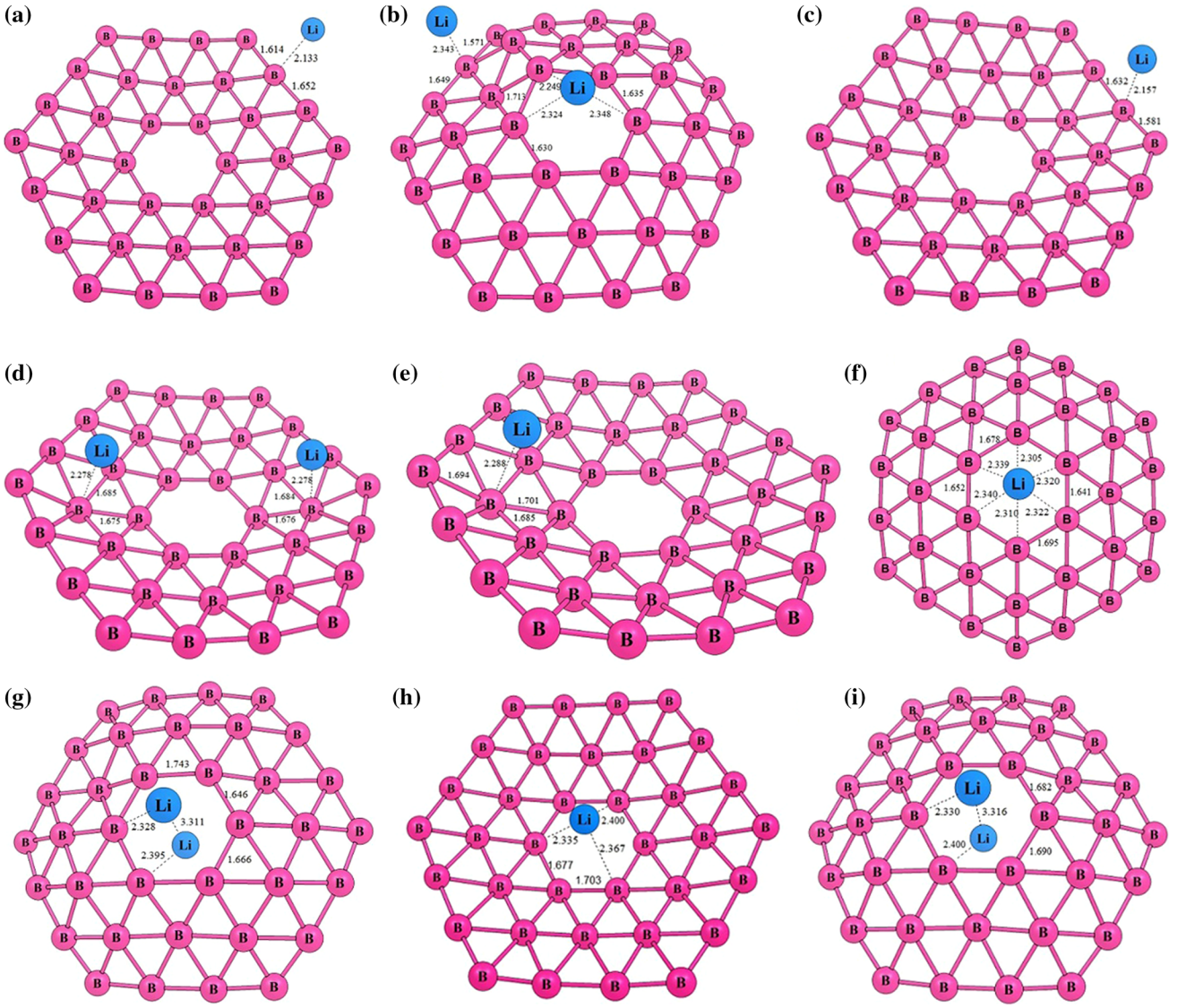

Fig. 2. The optimized geometry obtained structures for $Li_n@B_{36}$, (n = 1, 2) nanoclusters: (a) A, (b) B, (c) C, (d) D, (e) E, (f) F, (g) G, (h) H and (i) I structures. (These structures are arranged in order of decreasing in beta values).

Table II. The obtained natural electron configuration for the lithium atom in considered structures

Compound	Atom	Natural electron configuration
A	Li	[He] 2S(0.01)2p(0.02)
B	Li	[He] 2S(0.02)2p(0.07)
	Li	[He] 2S(0.01)2p(0.07)
C	Li	[He] 2S(0.02)2p(0.03)
D	Li	[He] 2S(0.02)2p(0.06)
	Li	[He] 2S(0.02)2p(0.06)
E	Li	[He] 2S(0.01)2p(0.05)
F	Li	[He] 2S(0.01)2p(0.07)
G	Li	[He] 2S(0.02)2p(0.11)
	Li	[He] 2S(0.03)2p(0.08)3p(0.01)
H	Li	[He] 2S(0.01)2p(0.02)
I	Li	[He] 2S(0.01)2p(0.05)
	Li	[He] 2S(0.01)2p(0.04)

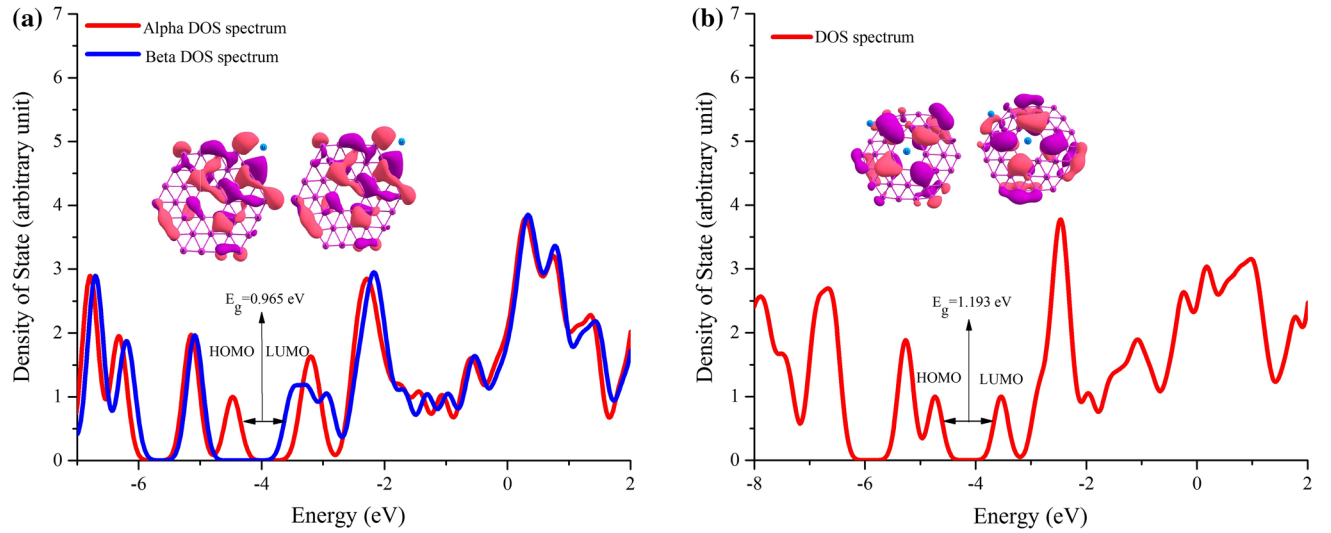

Fig. 3. Density of states (DOS) of (a) A, and (b) B structures.

considerable HLG reduction to 0.965 eV, implying significant interaction of the Li atom with the rim boron of B_{36} nanosheet. In order to provide a convenient comprehensive view of the electronic structures of the studied configurations, DOS and the pictorial representation of the HOMO–LUMO distribution of **A** and **B** structures are depicted in Fig. 3a and b. According to this figure, significant reduction in the HLG is due to the formation of a high-energy level as the new HOMO level locating between the original HOMO and LUMO of pristine B_{36}. Moreover, according to the results presented in Tables I as well as the DOS spectra, it can be concluded that stronger interaction of Li atom leads to enhancement in the HOMOs energy and, as such, gives a small HOMO–LUMO energy gap in studied clusters compared with pristine B_{36} nanosheet.

It has been shown that the existence of the diffuse excess electron can usually cause a large NLO response.[51,52] The obtained dipole moment (μ), polarizability (α) and first hyperpolarizability (β_0) of the considered systems are also listed in Table I. According to this table, the obtained outcomes show that polarizability and β_0 are enhanced due to adsorption of Li atoms. The results indicate that **A** and **B** structures have greatest first hyperpolarizability with the values 4920.62 and 1532.98 au, respectively, which indicates that β_0 values of $Li@B_{36}$ are larger than $Li_2@B_{36}$. In addition, the s valence electron of the Li atom is pushed out to turn into a diffuse excess electron for the whole system. It seems that the interaction distance between the Li atom and the B_{36} is a key factor in enhancing the first hyperpolarizability of the studied clusters. The shorter interaction distance causes the greater NLO response (see Fig. 2 and Table I). This observation is in agreement with results of previous studies on M@B40 (M = Li, Na, K).[39] The shortest interaction distances belong to the **A** configuration. Thus, it seems that the shorter interaction distance is responsible for greater NLO response of this structure among the studied clusters. It is obvious that rim boron of B_{36} is a favorable position for achieving considerable β_0 values. Finally, existence of the diffuse excess electron leads to large NLO response of $Li_n@B_{36}$ (n = 1, 2) nanoclusters with respect to B_{36} nanosheet.

CONCLUSION

In this study, we have investigated the alteration of NLO features of bowl-shape B_{36} nanosheet by interaction with lithium atom. It is found that these complexations narrow the HLGs of the considered structures. Such a decrease of the HLGs is mainly due to the formation of a high-energy level as the new HOMO levels locate between the original HOMO and LUMO of pristine nanosheet. The electronic properties of the studied structures are sensitive to interaction with the Li atom entirely. Indeed, the interaction of B_{36} with Li atom enhanced its first hyperpolarizability significantly. Finally, it is concluded that $Li_n@B_{36}$ (n = 1, 2) nanoclusters could be a potential promising NLO material.

REFERENCES

1. D.F. Eaton, in *Materials for Nonlinear Optics* (American Chemical Society, 1991), p. 128.
2. D.R. Kanis, M.A. Ratner, and T.J. Marks, *Chem. Rev.* 94, 195 (1994).
3. G. de la Torre, P. Vázquez, F. Agullo-Lopez, and T. Torres, *Chem. Rev.* 104, 3723 (2004).
4. O. Ostroverkhova and W. Moerner, *Chem. Rev.* 104, 3267 (2004).
5. K.B. Eisenthal, *Chem. Rev.* 106, 1462 (2006).
6. B.J. Coe, *Acc. Chem. Res.* 39, 383 (2006).
7. K. Okuno, Y. Shigeta, R. Kishi, and M. Nakano, *J. Phys. Chem. Lett.* 4, 2418 (2013).

8. S. Muhammad, H.-L. Xu, R.-L. Zhong, Z.-M. Su, A.G. Al-Sehemi, and A. Irfan, *J. Mater. Chem. C* 1, 5439 (2013).
9. R.-L. Zhong, H.-L. Xu, S. Muhammad, J. Zhang, and Z.-M. Su, *J. Mater. Chem.* 22, 2196 (2012).
10. C. Tu, G. Yu, G. Yang, X. Zhao, W. Chen, S. Li, and X. Huang, *Phys. Chem. Chem. Phys.* 16, 1597 (2014).
11. F. Zhou, J.-H. He, Q. Liu, P.-Y. Gu, H. Li, G.-Q. Xu, Q.-F. Xu, and J.-M. Lu, *J. Mater. Chem.* 100, 6850 (2014).
12. K. Hatua and P.K. Nandi, *J. Phys. Chem. A* 117, 12581 (2013).
13. S. Muhammad, H. Xu, and Z. Su, *J. Phys. Chem. A* 115, 923 (2011).
14. Y.-Y. Hu, S.-L. Sun, S. Muhammad, H.-L. Xu, and Z.-M. Su, *J. Phys. Chem. C* 114, 19792 (2010).
15. H.-Q. Wu, R.-L. Zhong, S.-L. Sun, H.-L. Xu, and Z.-M. Su, *J. Phys. Chem. C* 118, 6952 (2014).
16. P. Karamanis and C. Pouchan, *J. Phys. Chem. C* 116, 11808 (2012).
17. R.-L. Zhong, H.-L. Xu, Z.-R. Li, and Z.-M. Su, *J. Phys. Chem. Lett.* 6, 612 (2015).
18. W. Chen, Z.-R. Li, D. Wu, Y. Li, C.-C. Sun, and F.L. Gu, *J. Am. Chem. Soc.* 127, 10977 (2005).
19. G. Yu, X. Huang, S. Li, and W. Chen, *Int. J. Quantum Chem.* 115, 671 (2015).
20. S. Muhammad, H. Xu, Y. Liao, Y. Kan, and Z. Su, *J. Am. Chem. Soc.* 131, 11833 (2009).
21. G. Yu, X.R. Huang, W. Chen, and C.C. Sun, *J. Comput. Chem.* 32, 2005 (2011).
22. L.-J. Wang, S.-L. Sun, R.-L. Zhong, Y. Liu, D.-L. Wang, H.-Q. Wu, H.-L. Xu, X.-M. Pan, and Z.-M. Su, *RSC Adv.* 3, 13348 (2013).
23. E. Shakerzdeh, E. Tahmasebi, and H.R. Shamlouei, *Synt. Met.* 204, 17 (2015).
24. S. Kamalinahad, M. Solimannejad, and E. Shakerzadeh, *Bull. Chem. Soc. Jpn.* 89, 692 (2016).
25. F. Ma, Z.J. Zhou, and Y.T. Liu, *ChemPhysChem* 13, 1307 (2012).
26. E. Shakerzadeh, E. Tahmasebi, and Z. Biglari, *J. Mol. Liq.* 221, 443 (2016).
27. R.A. Èvarestov, *Theoretical Modeling of Inorganic Nanostructures: Symmetry and Ab Initio Calculations of Nanolayers, Nanotubes and Nanowires* (Berlin: Springer, 2015).
28. H. Dong, B. Lin, K. Gilmore, T. Hou, S.-T. Lee, and Y. Li, *Curr. Appl. Phys.* 15, 1084 (2015).
29. H. Bai, Q. Chen, H.J. Zhai, and S.D. Li, *Angew. Chem. Int. Ed.* 54, 941 (2015).
30. H.-J. Zhai, B. Kiran, J. Li, and L.-S. Wang, *Nat. Mater.* 2, 827 (2003).
31. A.P. Sergeeva, B.B. Averkiev, H.-J. Zhai, A.I. Boldyrev, and L.-S. Wang, *J. Chem. Phys.* 134, 224304 (2011).
32. Z.A. Piazza, W.-L. Li, C. Romanescu, A.P. Sergeeva, L.-S. Wang, and A.I. Boldyrev, *J. Chem. Phys.* 136, 104310 (2012).
33. Z.A. Piazza, H.-S. Hu, W.-L. Li, Y.-F. Zhao, J. Li, and L.-S. Wang, *Nat. Commun.* 5, 1 (2014).
34. H.J. Zhai, A.N. Alexandrova, K.A. Birch, A.I. Boldyrev, and L.S. Wang, *Angew. Chem. Int. Ed.* 42, 6004 (2003).
35. W. Huang, A.P. Sergeeva, H.-J. Zhai, B.B. Averkiev, L.-S. Wang, and A.I. Boldyrev, *Nat. Chem.* 2, 202 (2010).
36. H. Tang and S. Ismail-Beigi, *Phys. Rev. Lett.* 99, 115501 (2007).
37. E.S. Penev, S. Bhowmick, A. Sadrzadeh, and B.I. Yakobson, *Nano Lett.* 12, 2441 (2012).
38. X. Wu, J. Dai, Y. Zhao, Z. Zhuo, J. Yang, and X.C. Zeng, *ACS Nano* 6, 7443 (2012).
39. E. Shakerzadeh, Z. Biglari, and E. Tahmasebi, *Chem. Phys. Lett.* 654, 76 (2016).
40. S. Grimme, J. Antony, S. Ehrlich, and H. Krieg, *J. Chem. Phys.* 132, 154104 (2010).
41. S. Grimme, S. Ehrlich, and L. Goerigk, *J. Comput. Chem.* 32, 1456 (2011).
42. Y. Zhao and D.G. Truhlar, *Acc. Chem. Res.* 41, 157 (2008).
43. F. Ma, Z.-R. Li, Z.-J. Zhou, D. Wu, Y. Li, Y.-F. Wang, and Z.-S. Li, *J. Phys. Chem. C* 114, 11242 (2010).
44. R.L. Zhong, H.L. Xu, S.L. Sun, Y.Q. Qiu, and Z.M. Su, *Chem. Eur. J.* 18, 11350 (2012).
45. M.J. Frisch, G.W. Trucks, H.B. Schlegel, G.E. Scuseria, M.A. Robb, J.R. Cheeseman, G. Scalmani, V. Barone, B. Mennucci, G.A. Petersson, H. Nakatsuji, M. Caricato, X. Li, H.P. Hratchian, A.F. Izmaylov, J. Bloino, G. Zheng, J.L. Sonnenberg, M. Hada, M. Ehara, K. Toyota, R. Fukuda, J. Hasegawa, M. Ishida, T. Nakajima, Y. Honda, O. Kitao, H. Nakai, T. Vreven, J.A. Montgomery, Jr., J.E. Peralta, F. Ogliaro, M. Bearpark, J.J. Heyd, E. Brothers, K.N. Kudin, V.N. Staroverov, R. Kobayashi, J. Normand, K. Raghavachari, A. Rendell, J.C. Burant, S.S. Iyengar, J. Tomasi, M. Cossi, N. Rega, J.M. Millam, M. Klene, J.E. Knox, J.B. Cross, V. Bakken, C. Adamo, J. Jaramillo, R. Gomperts, R.E. Stratmann, O. Yazyev, A.J. Austin, R. Cammi, C. Pomelli, J.W. Ochterski, R.L. Martin, K. Morokuma, V.G. Zakrzewski, G.A. Voth, P. Salvador, J.J. Dannenberg, S. Dapprich, A.D. Daniels, O. Farkas, J.B. Foresman, J.V. Ortiz, J. Cioslowski, and D.J. Fox, *Gaussian 09, Revision A.02* (Wallingford, CT: Gaussian, Inc., 2009).
46. N.M. O'boyle, A.L. Tenderholt, and K.M. Langner, *J. Comput. Chem.* 29, 839 (2008).
47. A.D. Buckingham, *Adv. Chem. Phys.* 12, 107 (1967).
48. A. McLean and M. Yoshimine, *J. Chem. Phys.* 47, 1927 (1967).
49. S.F. Boys and F.D. Bernardi, *Mol. Phys.* 19, 553 (1970).
50. A.E. Reed, R.B. Weinstock, and F. Weinhold, *J. Chem. Phys.* 83, 735 (1985).
51. F.-F. Wang, Z.-R. Li, D. Wu, B.-Q. Wang, Y. Li, Z.-J. Li, W. Chen, G.-T. Yu, F.L. Gu, and Y. Aoki, *J. Phys. Chem. B* 112, 1090 (2008).
52. H.-L. Xu, Z.-R. Li, D. Wu, B.-Q. Wang, Y. Li, F.L. Gu, and Y. Aoki, *J. Am. Chem. Soc.* 129, 2967 (2007).